frontiers in Marine Science

ORIGINAL RESEARCH
published: 12 January 2022
doi: 10.3389/fmars.2021.760194

# Computed Microtomography (Micro-CT) in the Anatomical Study and Identification of Solenogastres (Mollusca)

*Jesús Martínez-Sanjuán[1*†], Kevin Kocot[2†], Óscar García-Álvarez[1†], María Candás[1†] and Guillermo Díaz-Agras[1†]*

*[1] REBUSC, Rede de Estacións Biolóxicas da Universidade de Santiago de Compostela, Estación de Bioloxía Mariña da Graña, Universidade de Santiago de Compostela, Santiago de Compostela, Spain, [2] Department of Biological Sciences and Alabama Museum of National History, University of Alabama, Tuscaloosa, AL, United States*

Solenogastres are vermiform marine molluscs characterised by an aculiferous mantle, a longitudinal ventral pedal groove and a terminal or subterminal pallial cavity. Their classification is based in part on the type of mantle sclerites, but identification to even the family level generally requires the study of internal anatomical characters. Taxonomically important internal characters include those related to radular structure, the type of ventrolateral glandular organs of the pharynx and the reproductive system, among others. In order to study their internal anatomical organisation, according to the classical reconstruction method, serial histological sections of specimens are made, from which the 2D internal anatomy of the specimen can be reconstructed manually. However, this is a time-consuming technique that results in destruction of the specimen. Computed microtomography or micro-CT is a non-destructive technique based on the measurement of the attenuation of X-rays as they pass through a specimen. Micro-CT is faster than histology for studying internal anatomy and it is non-destructive, meaning that specimens may be used for e.g., DNA extraction or retained as intact vouchers. In this paper, the utility of micro-CT for studying taxonomically important internal anatomical structures was assessed. Results of the 3D anatomical study of the soft parts of four specimens of three species using micro-CT are presented: *Proneomenia sluiteri* Hubrecht, 1880, *Dorymenia menchuescribanae* García-Álvarez et al., 2000 and *Anamenia gorgonophila* Kowalevsky, 1880. Micro-CT enabled detailed study of most taxonomically important anatomical characters, precise measurements of structures, and observation of the relative position of organs from a variety of angles. However, it was not possible to observe the radula and some details of the ventral foregut organs could not be discerned. Despite these limitations, results of this study highlight micro-CT as a valuable tool to compliment histology in the study of solenogaster anatomy and in non-destructively identifying animals to the family and even genus-level.

**Keywords: Solenogastres, micro-CT, anatomy, *Proneomenia sluiteri, Dorymenia menchuescribanae, Anamenia gorgonophila***

OPEN ACCESS

***Edited by:***
*Clara F. Rodrigues, University of Aveiro, Portugal*

***Reviewed by:***
*Ekin Tilic, University of Copenhagen, Denmark*
*Nina Therese Mikkelsen, University of Bergen, Norway*

****Correspondence:***
*Jesús Martínez-Sanjuán*
*jesmarsan14@gmail.com*

*† These authors have contributed equally to this work*

***Specialty section:***
*This article was submitted to Deep-Sea Environments and Ecology, a section of the journal Frontiers in Marine Science*

***Received:*** *17 August 2021*
***Accepted:*** *13 December 2021*
***Published:*** *12 January 2022*

***Citation:***
*Martínez-Sanjuán J, Kocot K, García-Álvarez Ó, Candás M and Díaz-Agras G (2022) Computed Microtomography (Micro-CT) in the Anatomical Study and Identification of Solenogastres (Mollusca). Front. Mar. Sci. 8:760194. doi: 10.3389/fmars.2021.760194*

## INTRODUCTION

Solenogastres are vermiform marine molluscs with no distinct head or other regionalisation. They are characterised by a mantle bearing calcareous scales or spines called sclerites, a longitudinal ventral pedal groove and a terminally or subterminally positioned pallial (= mantle) cavity. Knowledge about their biology is scarce and data on their diversity and geographic distribution are limited and uneven due to the fact that their study has been focused on restricted geographic areas, the difficulties of sampling and that many of the species have only been described from very few specimens. However, it cannot be said that they are rare animals as their presence extends from the coast to the deep sea (García-Álvarez et al., 2014).

To date, 293 species of Solenogastres have been described. They are grouped into four orders, whose classification is based primarily on the type of mantle sclerites. However, the order-level taxonomy of the group has been called into question (Kocot et al., 2019) and, for the classification of families, genera and species, it is essential to study their internal organisation in order to get to know the radular structure, the type of ventrolateral glandular organs of the pharynx and the other internal organs, especially the reproductive system (García-Álvarez and Salvini-Plawen, 2007).

In order to study the internal anatomical organisation, according to the classical reconstruction method, serial histological sections of specimens are made. From these, the internal anatomy may be reconstructed in a sagittal representation, obtaining a 2D anatomical view of the specimen. In addition, 3D computerised anatomical reconstruction can be performed by means of reconstruction software that stacks and aligns photographs of all the serial histological sections (Pedrouzo et al., 2019). Notably, this approach only works well for specimens embedded in resin, as paraffin sections tend to vary in their degree of compression, which makes image stacking and alignment challenging to impossible. Such 3D visualisation software offers the possibility of rotating, zooming in and out, and isolating different parts to observe different characters. Also, by not using fixed reference points, the distortion of the final image is reduced. However, histological sectioning and both manual and computerised anatomical reconstruction are highly labor-intensive and destructive approaches.

Computed microtomography or micro-CT is a non-destructive technique based on the measurement of the attenuation of X-rays when they pass through a sample while it rotates on itself (180° or 360°), resulting in a large number of radiographs (called X-ray projection images). From these projections, virtual 2D sections are obtained in the three planes (transverse, frontal and sagittal) comparable to histological ones, as well as 3D models that allow the external and internal structure of the scanned sample to be visualised. The advantage of this technique is that, as the sample is not destroyed, it is possible to carry out complementary studies at a later date. This is of paramount importance in Solenogastres where many species are rare and often only one specimen of a new species may be available. Whereas histology destroys the specimen and precludes other types of analysis, it is now possible to employ a workflow that collects data using light microscopy, micro-CT, scanning electron microscopy (SEM), and DNA barcoding all from the same specimen (Faulwetter et al., 2013b; Gignac et al., 2016). In addition, micro-CT eliminates possible image distortions, which are common in classical reconstruction methods.

The main aim of this work is to test the potential of micro-CT to describe the anatomy of the soft parts of Solenogastres. A description of the soft parts of each of the specimens is given based on the images obtained by micro-CT and some anatomical details are given in relation to the descriptions already published for each of the species and based on the data obtained by means of classical histological studies. The iconography of the anterior and posterior parts of *Proneomenia sluiteri* is completed in 3D micro-CT. In addition, the possibilities offered by this methodology for the study and identification of Solenogastres species are discussed. Regarding the sclerites of the mantle of Solenogastres, they are not discussed here, since their observation and study does not require the destruction of the specimens (García-Álvarez et al., 2014) and their calcareous nature is similar to the calcareous spicules of other marine molluscs already studied by this technique (Alba-Tercedor and Sánchez-Tocino, 2011; Paz-Sedano et al., 2021; Urgorri et al., 2021).

This paper presents the results of 3D anatomical study of the soft parts of one specimen of *Proneomenia sluiteri* Hubrecht, 1880, one specimen of *Dorymenia menchuescribanae* García-Álvarez et al., 2000 and two specimens of *Anamenia gorgonophila* Kowalevsky, 1880 using computed microtomography or micro-CT. Several studies have demonstrated the efficiency of this technique in the study of small marine molluscs (Golding and Jones, 2007; Alba-Tercedor and Sánchez-Tocino, 2011; Candás et al., 2016, 2017). Regarding Aplacophora, some experiments have been conducted with some species of Solenogastres (Candás et al., 2018; Pedrouzo et al., 2019) and Caudofoveata (Metscher, 2009).

## MATERIALS AND METHODS

Four specimens representing three described species of a size suitable for this first comparative study were studied: one specimen of *Proneomenia sluiteri* Hubrecht, 1880 from East Iceland, one specimen of *Dorymenia menchuescribanae* García-Álvarez et al., 2000 from South Shetland Islands, Antarctica and two specimens of *Anamenia gorgonophila* Kowalevsky, 1880 one from Reykjanes Ridge, Iceland and one from Alborán Sea, South Iberian Peninsula.

The four specimens, which were fixed and preserved in 70% ethanol, were subjected to alcoholic dehydration by ethanol baths (80, 90, and 96%) for 24 h each. The two *A. gorgonophila* specimens were then stained with iodine in 96% ethanol for 3 days and dehydrated with Hexamethyldisilazane (HMDS) and air dried overnight. The specimens of *P. sluiteri* and *D. menchuescribanae* were stained with iodine in 96% ethanol for 1 week, dehydrated with HMDS and left to dry overnight. Prior to dehydration with HDMS, specimens were rinsed with 96° ethanol to remove excess iodine. Hexamethyldisilizane (HDMS) removes water from tissues effectively increasing the clarity of boundaries between air and tissue which in turn enhances the

contrast when scanning with X-rays (Paterson et al., 2014). The use of HDMS improves image quality by avoiding artifacts caused during scanning of samples in liquid (Faulwetter et al., 2013a; Keklikoglou et al., 2019).

The four specimens studied were previously scanned without any staining. The images obtained are not presented in this article because they are not of sufficient quality to be able to study the internal anatomy.

The specimens were scanned on a Skyscan 1172 microtomograph (Bruker, Belgium) applying the parameters: 55 kv, 165 μA and 360° sample rotation. Pixel sizes were 6.78 μm for the *P. sluiteri* specimen, 5.97 μm for the *D. menchuescribanae* specimen and between 2.98 and 4.95 μm for the *A. gorgonophila* specimens.

NRecon software (Bruker, Belgium) was used to reconstruct the X-ray projection images obtained during scanning, resulting in 2D sections. Subsequently, CTAn and DataViewer software (Bruker, Belgium) were used to obtain cross-sectional, frontal and sagittal sections, as well as to clean the images. Finally, three-dimensional models of each of the scanned specimens were made using CTVox software (Bruker, Belgium).

Datasets of transverse 2D images of studied specimens were uploaded to Morphosource[1].

## RESULTS

**(Classification following: García-Álvarez and Salvini-Plawen, 2007)**

Order **CAVIBELONIA** Salvini-Plawen (1978)

Family **PRONEOMENIIDAE** Simroth and Bronn (1893)

### Genus *Proneomenia* Hubrecht, 1880

***Proneomenia sluiteri*** Hubrecht, 1880

**Material examined:** 1 specimen. East Iceland, Norwegian Sea. ICEAGE (66°17′43″N, 12°21′45″W—66°18′06″N, 12°22′37″W), Meteor M85/3, Area 30. 662–729 m deep (**Figures 1–6**).

Habitus: Body elongated, circular in section (36 mm long, 5 mm in average diameter), with a slight narrowing in its anterior and posterior regions, being more pronounced in the latter (**Figure 1A**). No keels or papillae on the mantle surface. The openings of the atriobuccal cavity (Abc, **Figure 1B**) (1 mm long) at the anterior end of the body and of the pallial cavity (Pc, **Figure 1D**) (3 mm long) at the posterior end are well visible. The pedal groove (Pg, **Figures 1A,B,D**, **3D,F**, **6D,F**) is well visible externally (24 mm long), running ventrally from the pedal pit (Pp, **Figures 1B**, **3B,C**), located posterior to the atriobuccal opening, up to the opening of the pallial cavity. No sclerites attached to the pedal groove are visible.

Mantle: Cuticle 250 μm thick (Cu, **Figures 2A**, **3A,C,E**). No tegumentary excrescences or sclerite formations toward the outside of the mantle.

Pallial cavity: The cavity (4 mm long, 2 mm high and 2 mm wide) opens to the outside through a long and wide opening (3 mm long and 700 μm wide) in the ventroposterior area of the body (Pc, **Figures 4**, **5**, **6A**). The pallial cavity bears two groups of abdominal spicules (Ab, **Figures 4B**, **5C,E,F**, **6B,C**), located on either side of the opening of the pallial cavity, extending 2 mm in length and running laterally to the pallial cavity itself. The rectum (Re, **Figures 4B**, **5A,E,F**, **6B–D**) opens into the anus (1 mm in diameter) located on the dorsorrostral wall of the cavity. Ventrally to the rectum, the unpaired opening of the spawning ducts (1 mm in diameter) is located (Sd, **Figures 4A**, **5**, **6C,D**). Diverticula (Di, **Figures 5A,B,D**, **6A**), nor respiratory folds, are observed in the dorsoposterior region of the pallial cavity.

Digestive system: The atriobuccal cavity (Abc, **Figures 2A,C**) (3 mm long, 1.5 mm wide and 2 mm high), opens to the outside through an opening in the ventroanterior region of the body (1 mm long and 300 μm wide). The posterior wall of the atriobuccal cavity contains the mouth, which is oval (1.5 mm high and 2 mm wide). The pharynx (Ph, **Figures 2**, **3A**) is short, wide and circular in section (4 mm long and 1 mm in diameter), covered internally by a thick cuticle (150 μm thick) and bears glands on the dorsal wall. The ventral glandular organs of the pharynx (Vfg, **Figures 2**, **3B–D,E**) lead to the ventroposterior pharyngeal area, anterior to the radular sac (Rs, **Figures 2**, **3B,C**). These glandular organs are of type C (García-Álvarez and Salvini-Plawen, 2007), consisting of two ducts (11 mm long and 0.6 mm in diameter) whose lumen is not delimited by a muscular wall and run ventrally to the intestine (Vfg, **Figures 3D,E**). The oesophagus (Oe, **Figures 2**, **3B–D**) is 3 mm long and of the same diameter as the pharynx. The oesophagus leads dorsorostrally and slightly ventrally into the intestine (Oe, **Figures 2A**, **3D**). From the dorsoanterior region of the intestine, a long, dorsoventrally flattened dorsal caecum (Dc, **Figures 2A,B**, **3A–C**) (6 mm long, 1 mm wide and 0.5 mm high) projects anteriorly, reaching into the area of the atriobuccal cavity. The intestine (Mg, **Figures 2A,B**, **3D,E**) occupies most of the interior of the animal (22 mm long and 2.5 mm in average diameter), its inner walls show folds and remains of Alcyonacea (Al, **Figures 2C**, **3F**). The folds formed by the dorsoventral musculature (Dvm, **Figures 2B,C**, **3D,E**, **4**, **5A**) along the length of the intestine can be seen. The intestine continues into the rectum (Re, **Figures 4B**, **5A,D–F**, **6B–D**), 1 mm in diameter, and opens into an anus, circular (1 mm in diameter) located dorsorrostrally in the pallial cavity.

Sense organs: The atrial region (At, **Figures 2A,B**) (1 mm long, 1.5 mm wide and 2 mm high) is located in the dorsoanterior area of the atriobuccal cavity and bears narrow-necked sensory papillary protrusions attached directly to the anterior, dorsal and lateral walls of the atrium. The specimen bears a dorsoterminal sense organ (Dso, **Figures 1C**, **4B**, **5E**, **6B**), located in the midline of the body, at the level of the pallial cavity.

Gonopericardial system: The pair of gonads (Go, **Figures 2**, **3F**, **4A**) (18 mm long and 1 mm in diameter) are filled with oocytes, situated on both sides of the thin central septum separating the two gonads. The gonads are attached to the pericardium (Pr, **Figure 4**) through two gonopericardioducts (Gd, **Figures 4**, **6F**) (1 mm long and 100 μm in diameter). The pericardium (Pr, **Figures 4**, **5F**, **6D,E**) is wide and slightly narrowed dorsoventrally (4 mm long, 2.5 mm at its maximum

[1]https://www.morphosource.org/projects/000384772

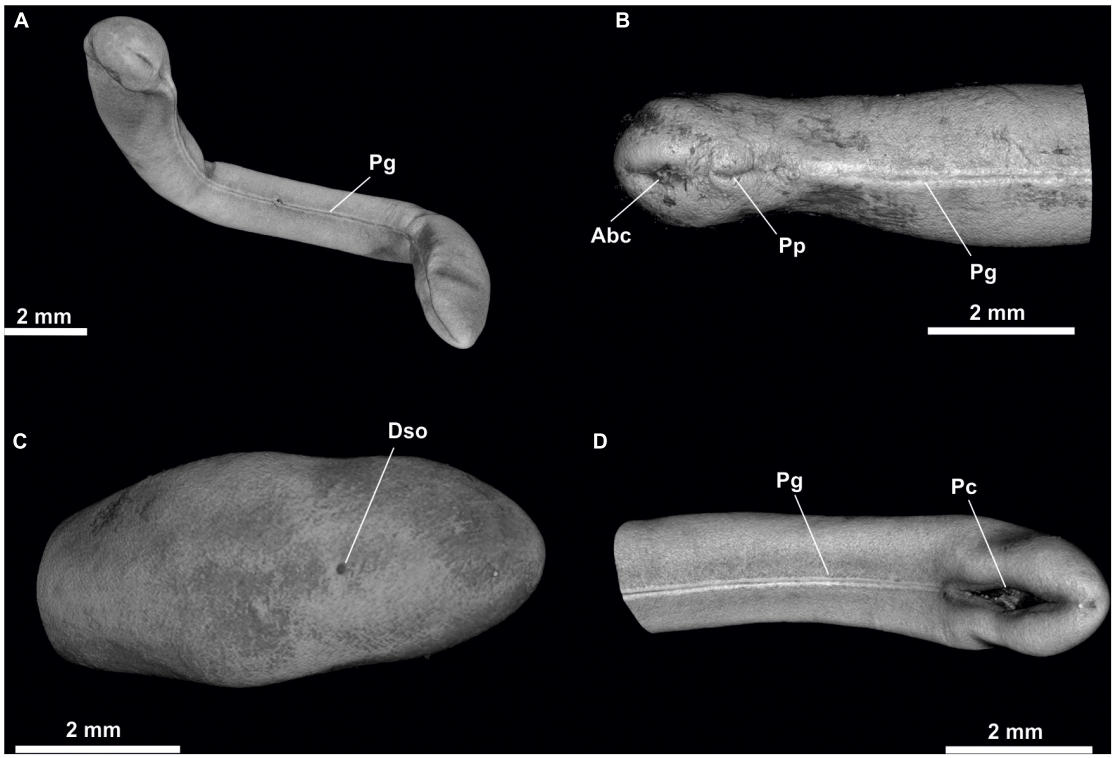


**FIGURE 1 |** *Proneomenia sluiteri*. **(A)** Habitus. **(B)** Anterior body. **(C)** Posterior body from dorsal view. **(D)** Posterior body from ventral view. Abc, Atriobuccal cavity; Dso, Dorsoterminal sense organ; Pc, Pallial cavity; Pg, Pedal groove; Pp, Pedal pit.

width and 2 mm high); oocytes are visible inside (**Figures 4**, **6D,E**). The heart (Ht, **Figures 4**, **6D,E**), located in the dorsal wall of the pericardium, is an elongated and narrow chamber (3 mm long and 100 μm in diameter). The two pericardioducts (Pd, **Figures 4A**, **5A,B**, **6C–F**) (5 mm long and 100 μm in diameter) originate from the posterior region of the pericardium, which first run briefly toward the posterior region of the body and then turn and run anteriorly, until they lead to the anterior region of the spawning ducts (Pd, Sd, **Figures 5E**, **6F**). There is a pair of elongated, undulating seminal receptacles (Sr, **Figures 5A,B,D,F**; **6E**) (3 mm long, 200 μm in diameter), attached to the pericardioducts through a short tube (150 μm long, 50 μm in diameter) located at the junction of the pericardioducts with the spawning ducts. The pair of spawning ducts (Sd, **Figures 4**, **5A,B,D–F**, **6C–F**) (4.5 mm long, 900 μm in diameter) merge posteriorly into a short, wide duct (600 μm long, 1 mm in diameter) that leads onto the rostral wall of the pallial cavity, ventrally to the rectum (Sdo, **Figure 6B**).

## Genus Dorymenia Heath, 1911

***Dorymenia menchuescribanae*** García-Álvarez et al., 2000

Material examined: 1 specimen of the type material (paratype 1. Collection of Estación de Bioloxía Mariña da Graña. Ferrol. Spain). South of Livingston Island, South Shetland Islands, Antarctica. BENTART-94 (62°43′24″S, 60°26′34″W), Station 71-R. 50 m deep (García-Álvarez et al., 2000) (**Figures 7–11**).

Habitus: Elongated body, circular in section (45 mm long and 4.5 mm in diameter), tapering at the anterior and posterior ends (**Figure 8**). No keels or papillae protruding from the mantle surface. The openings of the atriobuccal cavity (1 mm long) (Abc, **Figure 7B**) and of the pallial cavity (1.5 mm long) are well visible (Pc, **Figure 7D**). The pedal groove (**Figure 7D**) is visible externally (40 mm long), and runs along the ventral region of the animal from the pedal pit (Pp, **Figure 8A**), situated posterior to the atriobuccal cavity, until it enters the pallial cavity.

Mantle: Cuticle 200–300 μm thick. No outward projections of sclerites or other structure protruding from the mantle.

Pallial cavity: The cavity (2 mm long, 1.5 mm wide and 1 mm high) (**Figures 9**, **10A**, **11A,B,D**) opens to the outside through an elongated and wide opening (1.5 mm long and 100 μm wide) located in the ventroposterior area of the body (**Figure 7D**). The pallial cavity has abdominal sclerites located along almost the entire length of the opening of the pallial cavity (1 mm in extent). The pallial cavity has, in its dorsoanterior part, two sacs or compartments (**Figure 9B**); the dorsal sac is wider (700 μm long, 1.5 mm high and 1.5 mm wide) than the ventral one (400 μm long, 800 μm and 800 μm high). In the dorsal sac, the rectum (Re, **Figures 9B**, **10B**) opens into the anus (1.5 mm in diameter) located dorsorrostrally; and on the rostral wall of the ventral sac is the unpaired opening of the spawning ducts (700 μm in diameter) (Sd, **Figures 9B**, **10B**). The pallial cavity also bears a pair of 1 mm long copulatory stylets (Co, **Figures 9A**, **10A**, **11A,E**), with strong musculature surrounding them; the


**FIGURE 2 |** *Proneomenia sluiteri*. Anterior body. **(A)** Sagittal view. **(B)** Frontal-sagittal view. **(C)** Ventral view. Abc, Atriobuccal cavity; Al, Alcyonacea; At, Atrium; Cu, Cuticle; Dc, Dorsal caecum; Dvm, Dorsoventral musculature; Go, Gonad; Mg, Midgut; Oe, Oesophagus; Ph, Pharynx; Rs, Radular sac; Vfg, Ventral foregut glands.

stylets are situated ventrolaterally to the pallial cavity and run slightly diagonally from the anterior region of the cavity to its central region. The pallial cavity has diverticula in its dorsal wall (Di, **Figures 9**, **10A**, **11B,D**). The pallial cavity bears no respiratory folds.

Digestive system: The atriobuccal cavity (2 mm long, 1 mm wide and 1 mm high) (Abc, **Figure 8A**) opens to the outside through an opening 1 mm long, located in the ventroanterior region of the body (Abc, **Figure 7B**). On the posterior wall of the atriobuccal cavity is the circular mouth (1 mm in diameter). The

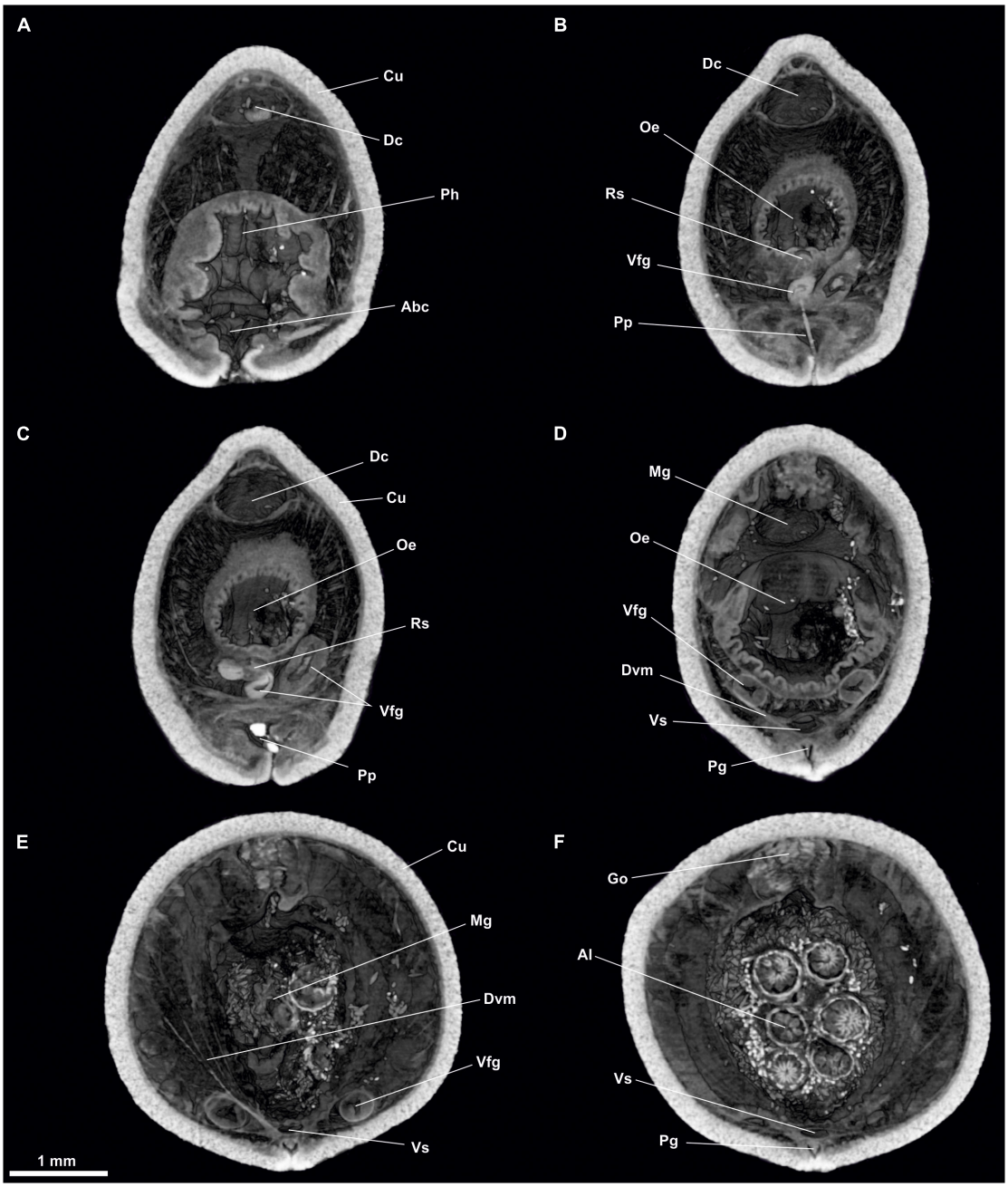


**FIGURE 3 |** *Proneomenia sluiteri*. Anterior body. **(A)** Cross-section through the atriobuccal cavity. **(B–D)** Cross-section through the oesophagus. **(E,F)** Cross-section through the midgut. Abc, Atriobuccal cavity; Al, Alcyonacea; Cu, Cuticle; Dc, Dorsal caecum; Dvm, Dorsoventral musculature; Go, Gonad; Mg, Midgut; Oe, Oesophagus; Pg, Pedal groove; Ph, Pharynx; Pp, Pedal pit; Rs, Radular sac; Vfg, Ventral foregut glands; Vs, Ventral senus.

pharynx (Ph, **Figure 8**) is 4 mm long and 0.8 mm in diameter, has a thick cuticle (100 μm thick) accompanied by glands. In the ventroposterior region of the pharynx, the ventral glandular organs of the pharynx (Vfg, **Figure 8**) end, slightly anterior to the radular sac (Rs, **Figure 8**). These organs are of type C (García-Álvarez and Salvini-Plawen, 2007), consisting of a pair of ducts 30 mm long and 0.5 mm in diameter, whose lumen is not delimited by a muscular wall, and run ventrally to the intestine. The pharynx joins ventrally to the intestine, it lacks an oesophagus. From the anterodorsal region of the intestine, the dorsoanterior caecum (Dc, **Figure 8A**) projects, slightly flattened dorsoventrally (2 mm long, 600 μm wide and 200 μm high) and reaches the height of the atriobuccal cavity. The intestine (Mg, **Figures 8**, **9**, **11A,D**) continues along the body (30 mm long and 2 mm in diameter); rest of Octocorallia (Oc **Figures 9B**, **10B**, **11D**) are observed up to the rectum (2 mm long and 1.5 mm in


**FIGURE 4 |** *Proneomenia sluiteri*. Posterior body. **(A)** Sagittal view through the spawining duct. **(B)** Sagittal view through the rectum. Ab, Abdominal spicules; Al, Alcyonacea; Dso, Dorsoterminal sense organ; Dvm, Dorsoventral musculature; Gd, Gonopericardioduct; Go, Gonad; Ht, Heart; Mg, Midgut; Ov, Oocyte; Pc, Pallial cavity; Pd, Pericardioduct; Pr, Pericardium; Re, Rectum; Sd, Spawning duct.

diameter) which runs into the anus (1.5 mm in diameter), located in the dorsorrostral wall of the pallial cavity.

Sense organs: Atrium (At, **Figure 8**) of small size (1 mm long, 1 mm wide and 1 mm high), located in the anterior part of the atriobuccal cavity, has a preatrial sense organ (Po, **Figure 8A**) located on the anterior wall of the atrium and sensory papillae on the anterior and lateral walls. The specimen bears a dorsoterminal sense organ (Dso, **Figures 7A,C**, **11B**) located in the dorsal midline of the body, at the end of the pallial cavity, visible externally.

Gonopericardial system: The pair of gonads (Go, **Figures 8B**, **9B**) (28 mm long and 1.5 mm in diameter) have oocytes on the thin septum that separates them. The gonads are attached to the pericardium by a pair of gonopericardioducts (Gd, **Figure 9B**) (1.5 mm long and 200 μm in diameter). The pericardium (Pr, **Figures 9B**, **10**, **11E**) is broad (2 mm long, 1 mm wide and 0.5 mm high); the elongated and narrow heart (2 mm long and 100 μm in diameter) lies on its dorsal wall. The pericardium extends posteriorly into two compartments, from which the two pericardioducts originate (Pd, **Figure 11C**), which first run toward the posterior region of the body and then turn and run anteriorly along the lateral regions of the body (3 mm long and 100 μm in diameter) until they lead to their respective spawning ducts (**Figures 9A**, **11B,D,E**). The specimen has a pair of spherical seminal receptacles (Sr, **Figures 9A**, **10A**, **11D**) (400 μm in diameter) located anterior to each spawning

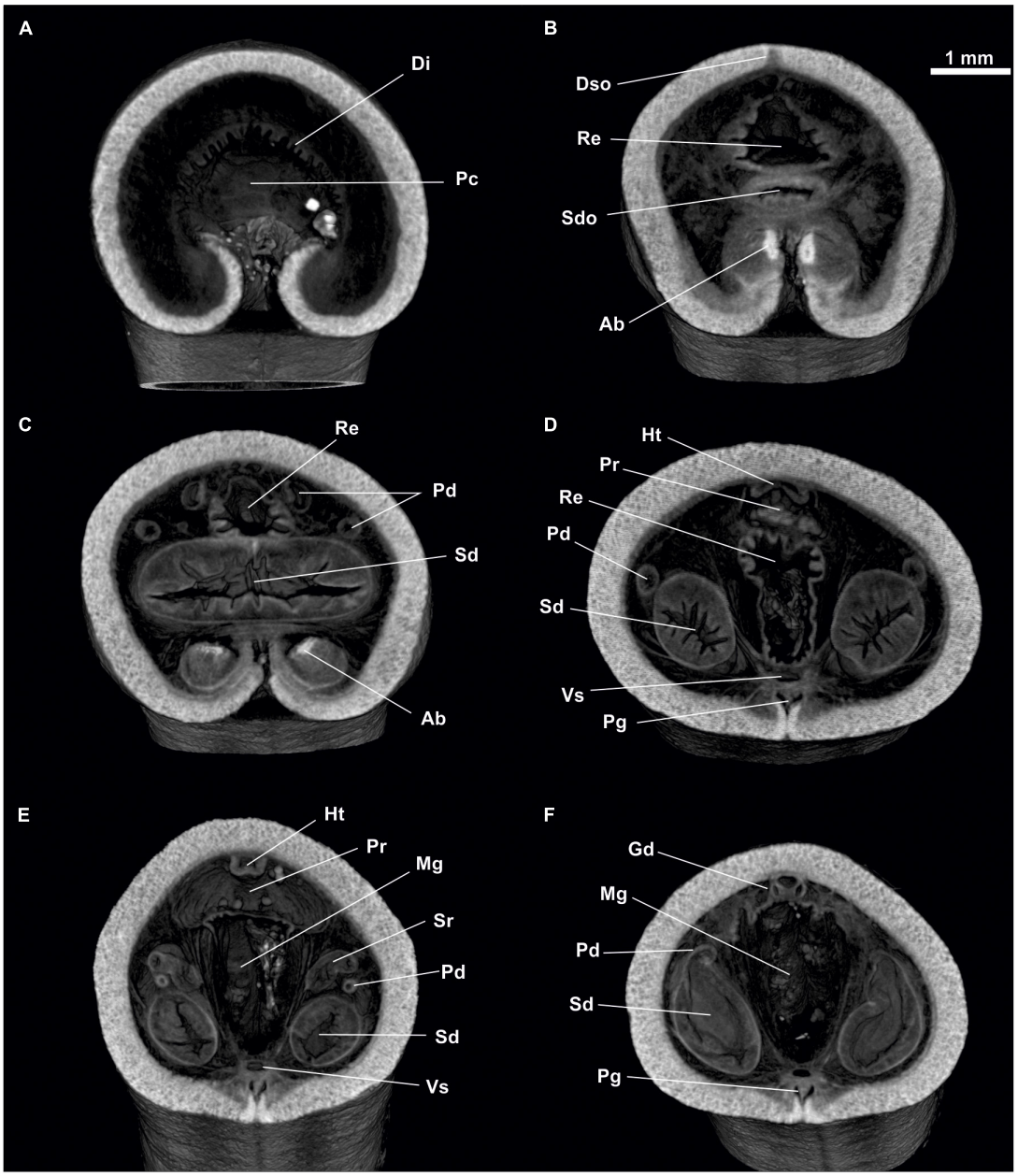


**FIGURE 5 |** *Proneomenia sluiteri*. Posterior body. **(A)** Cross-section through the pallial cavity. **(B)** Cross-section through the spawining duct opening. **(C–F)** Cross-section through the spawining duct. Ab, Abdominal spicules; Di, Diverticles; Dso, Dorsoterminal sense organ; Gd, Gonopericardioduct; Ht, Heart; Mg, Midgut; Pc, Pallial cavity; Pd, Pericardioduct; Pg, Pedal groove; Pr, Pericardium; Re, Rectum; Sd, Spawning duct; Sdo, Spawning duct opening; Sr, Seminal receptacles; Vs, Ventral sinus.

duct and attached to them through a narrow duct (300 μm long and 50 μm in diameter) in the area where the spawning ducts join the pericardioducts. The spawning ducts (**Figures 9**, **10**, **11A,C,D,E**), 2 mm long and 600 μm in diameter, continue toward the posterior region until they merge into a single duct 300 μm long and 700 μm in diameter, which leads to the rostral wall of the ventral sac of the pallial cavity (**Figures 9B**, **10B**, **11**).

**Family STROPHOMENIIDAE Salvini-Plawen, 1978**

## Genus *Anamenia* Nierstrasz, 1908

***Anamenia gorgonophila*** Kowalevsky, 1880

**Material examined:** 1 specimen. Reykjanes Ridge, Iceland. ICEAGE (60°16′55″N, 29°19′08″W), MSM 75, DZMB-HH 61716, station 188. 646 m deep (**Figure 12**).

Habitus: Body elongate, slightly narrowed laterally (30 mm long, 1.5 mm wide and 2 mm high), flattened ventrally and with narrower anterior and posterior ends. Surface irregular,

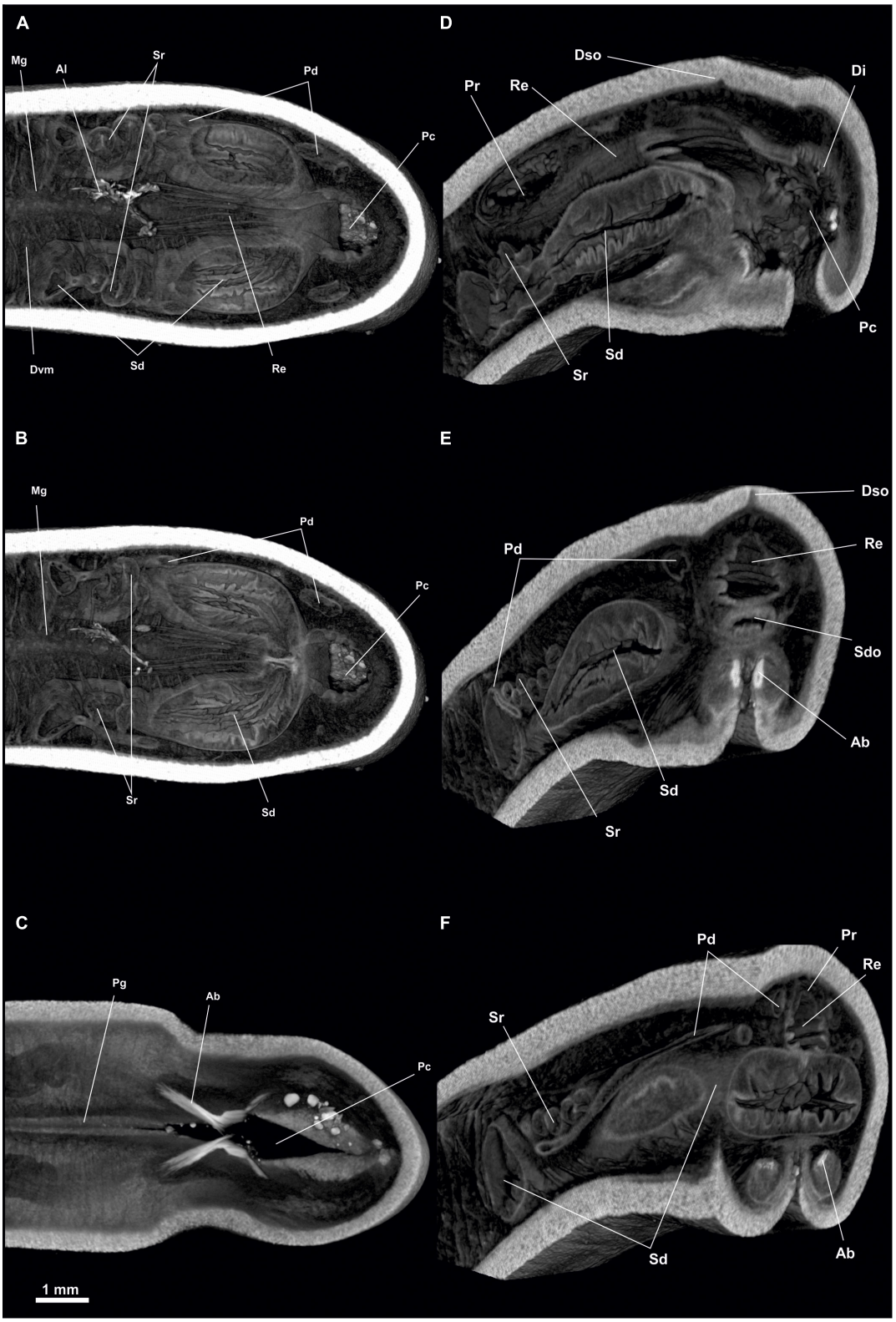


**FIGURE 6 |** *Proneomenia sluiteri*. Posterior body. **(A)** Dorsal view through the rectum. **(B)** Dorsal view through the spawning duct. **(C)** Dorsal view through the abdominal spicules. **(D–F)** Frontal-sagittal view Ab, Abdominal spicules; Al, Alcyonacea; Di, Diverticles; Dso, Dorsoterminal sense organ; Dvm, Dorsoventral musculature; Mg, Midgut; Pc, Pallial cavity; Pd, Pericardioduct; Pg, Pedal groove; Re, Rectum; Sd, Spawning duct; Sdo, Spawning duct opening; Sr, Seminal receptacles.

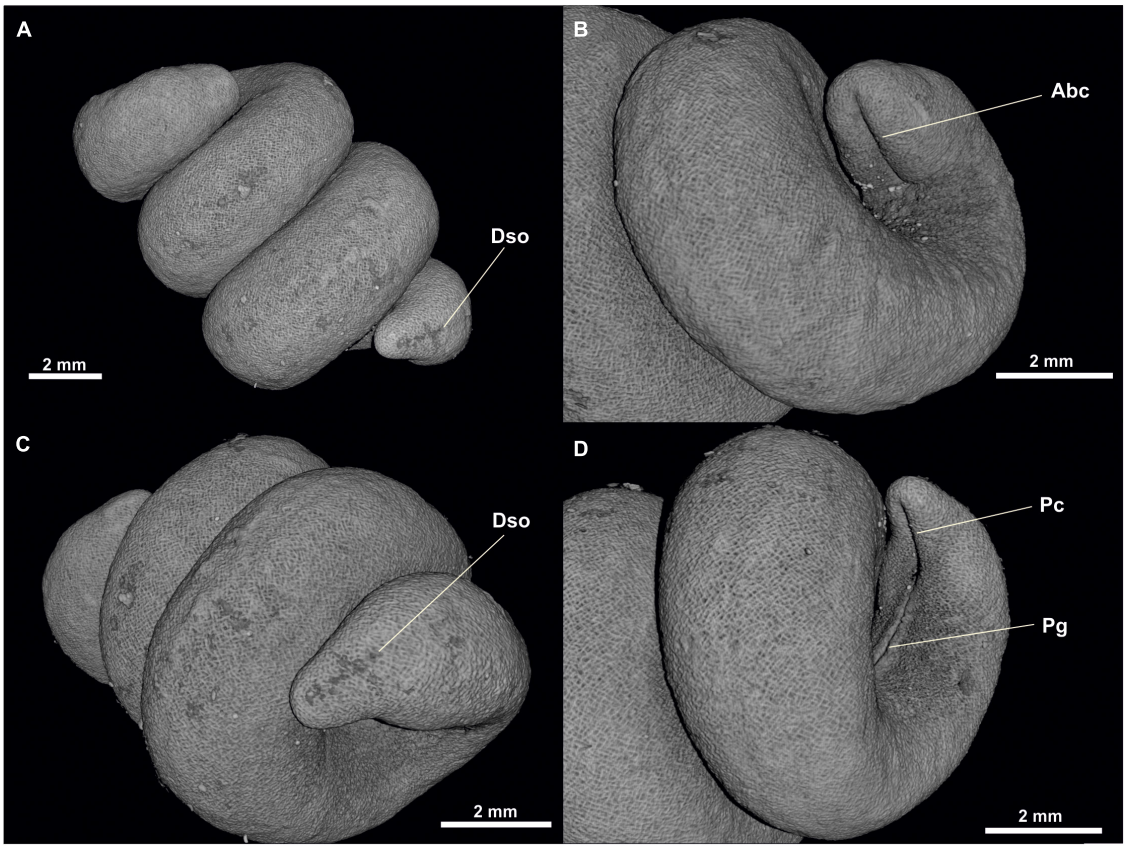


**FIGURE 7 |** *Dorymenia menchuescribanae*. **(A)** Habitus. **(B)** Anterior body from ventral view. **(C)** Posterior body from dorsal view. **(D)** Posterior body from ventral view. Abc, Atriobuccal cavity; Dso, Dorsoterminal sensitive organ; Pc, Pallial cavity; Pg, Pedal groove.

with acicular sclerites protruding from the mantle surface (**Figure 12A**), giving the animal a hirsute appearance. Pedal groove (Pg, **Figure 12A**) visible (20 mm long), with spicules on both sides, running along the ventral region of the animal from the pedal pit, situated posterior to the atriobuccal cavity, up to the pallial cavity without entering it.

Mantle: Cuticle 100–150 μm thick. With criss-crossed acicular sclerites and some protruding from the mantle surface. No integumentary structures such as keels or papillae. Long scales on both sides of the peduncle furrow along its entire length.

Pallial cavity.- The cavity (1 mm long and 700 μm in diameter) opens to the exterior through a 1 mm long opening in the ventroposterior region of the body (Pc, **Figure 12C**). The pallial cavity bears diverticula on the dorsal and lateral walls of the pallial cavity. The anus (400 μm in diameter) opens dorsorostrally and the spawning ducts (Sd, **Figure 12C**) (200 μm in diameter each) open paired and ventrally to it. The pallial cavity has a small ventrorrostral sac (200 μm long, 100 μm wide and 50 μm high) ventrally to the openings of the spawning ducts.

Digestive system.- The atriobuccal cavity (500 μm long and 250 μm in diameter) opens to the exterior through a 400 μm long opening and is located in the ventroanterior region of the body. The mouth occupies the posterior wall of the atriobuccal cavity and is circular (250 μm in diameter). The pharynx (Ph, **Figure 12B**) is long, circular in section (2.5 mm long and 200 μm in diameter) and covered by a thin cuticle (25 μm thick). The ventral glandular organs of the pharynx lead into the ventroposterior region of the pharynx, anterior to the radular sac. These organs are of type B (García-Álvarez and Salvini-Plawen, 2007) and are formed by a pair of serpentine ducts 8 mm long and 100 μm in diameter, whose lumen is delimited by a muscular wall, and run ventrally to the intestine. The pharynx joins ventrally the intestine (Mg, **Figure 12B**) and bears no oesophagus. From the anterodorsal region of the intestine, the caecum (Dc, **Figure 12B**) projects dorsoanteriorly (2 mm long, 200 μm wide and 100 μm high) reaching the height of the atriobuccal cavity. The intestine continues along the body (22 mm long and 1 mm in diameter), with remains of gorgonians inside. The folds formed by the dorsoventral musculature (Dvm, **Figure 12B**) along the intestine are clearly visible. The intestine is followed by the rectum (1 mm long and 400 μm in diameter), which leads to the anus (400 μm in diameter), located in the dorsorrostral wall of the pallial cavity.

Sense organs.- Atrium 200 μm long, 250 μm wide and 250 μm high (At, **Figure 12B**), occupying the anterior region of the atriobuccal cavity, with sensory papillary projections on its anterior, dorsal and lateral walls. The specimen bears a dorsoterminal sense organ (Dso, **Figure 12C**) in the dorsal midline of the body, at the level of the end of the pallial cavity, not visible externally.

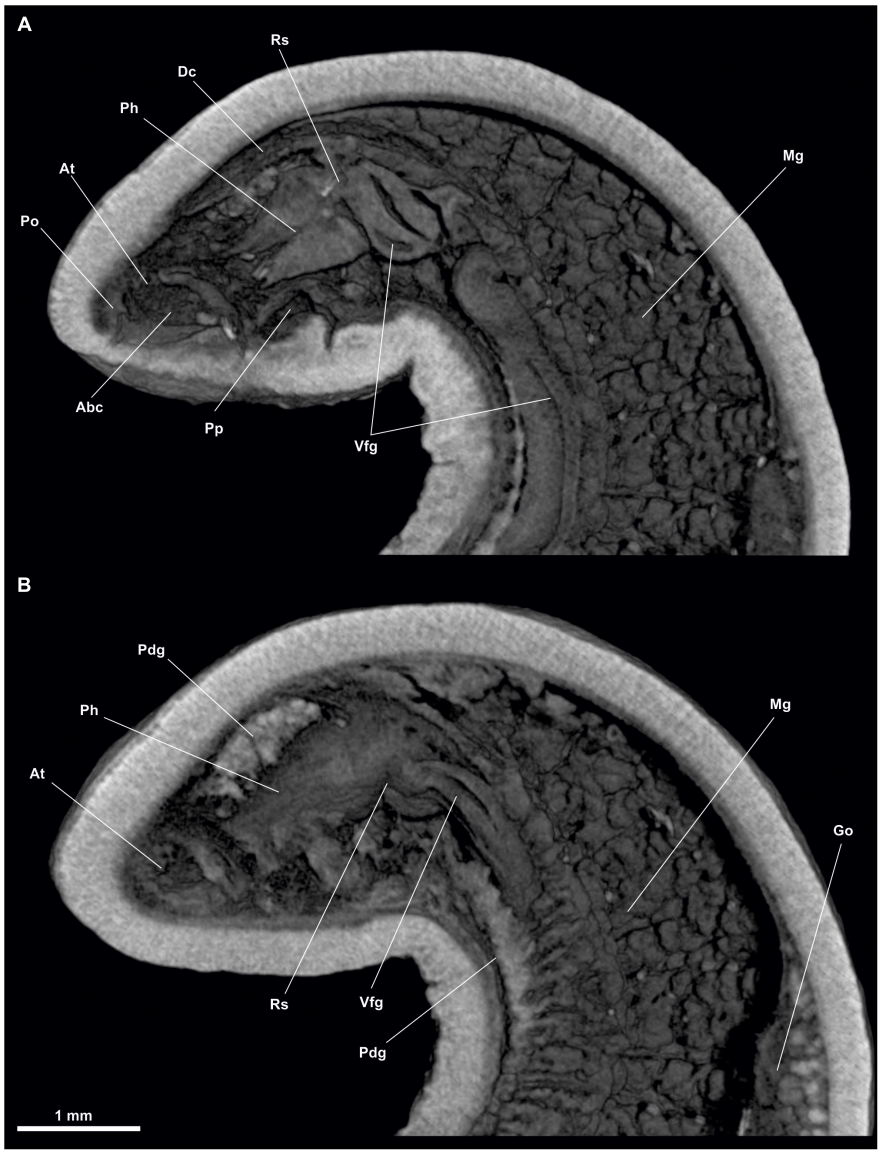


**FIGURE 8 |** *Dorymenia menchuescribanae*. **(A,B)** Sagittal views of the anterior body. Abc, Atriobuccal cavity; At, Atrium; Dc, Dorsal caecum; Go, Gonad; Mg, Midgut; Pdg, Pedal gland, Ph, Pharynx; Po, Preatrial organ; Pp, Pedal pit; Rs, Radular sac; Vfg, Ventral foregut glands.

Gonopericardial system.- The pair of gonads (Go, **Figure 12B**) (20 mm long and 400 μm in diameter) have oocytes on the septum separating them. A pair of gonopericardioducts (200 μm long and 100 μm in diameter) join the gonads to the pericardium. The pericardium is broad (1.5 mm long and 1 mm in diameter) with oocytes inside; on its dorsal wall, the heart is elongated and narrow (1 mm long and 80 μm in diameter). The posterior region of the pericardium extends into two compartments, from which the two pericardioducts emerge from a terminal lateral position, run toward the posterior region of the body, turn and run anteriorly along the lateral regions of the body (1.5 mm long and 60 μm in diameter), until they lead (Sd, **Figure 12C**) to each spawning duct. The seminal receptacles (Sr, **Figure 12C**) (together measuring 400 μm long and 300 μm in diameter) lead in bundles into the anterior region of each spawning duct. The two spawning ducts (Sd, **Figure 12C**) are slightly flattened (1 mm long, 200 μm wide and 100 μm high) and extend posteriorly until they each end individually (Sdo, **Figure 12C**) at the rostral wall of the pallial cavity, ventral to the rectum and dorsal to the ventrorrostral sac of the cavity.

## *Anamenia gorgonophila* Kowalevsky, 1880

**Material examined:** 1 specimen. Alboran Sea (South Iberian Peninsula). FAUNA IBÉRICA IV (35°50′01″N, 03°15′13″E–35°49′46″N, 03°14′27″E), Station 316. 90–240 m depth (**Figures 13–15**).

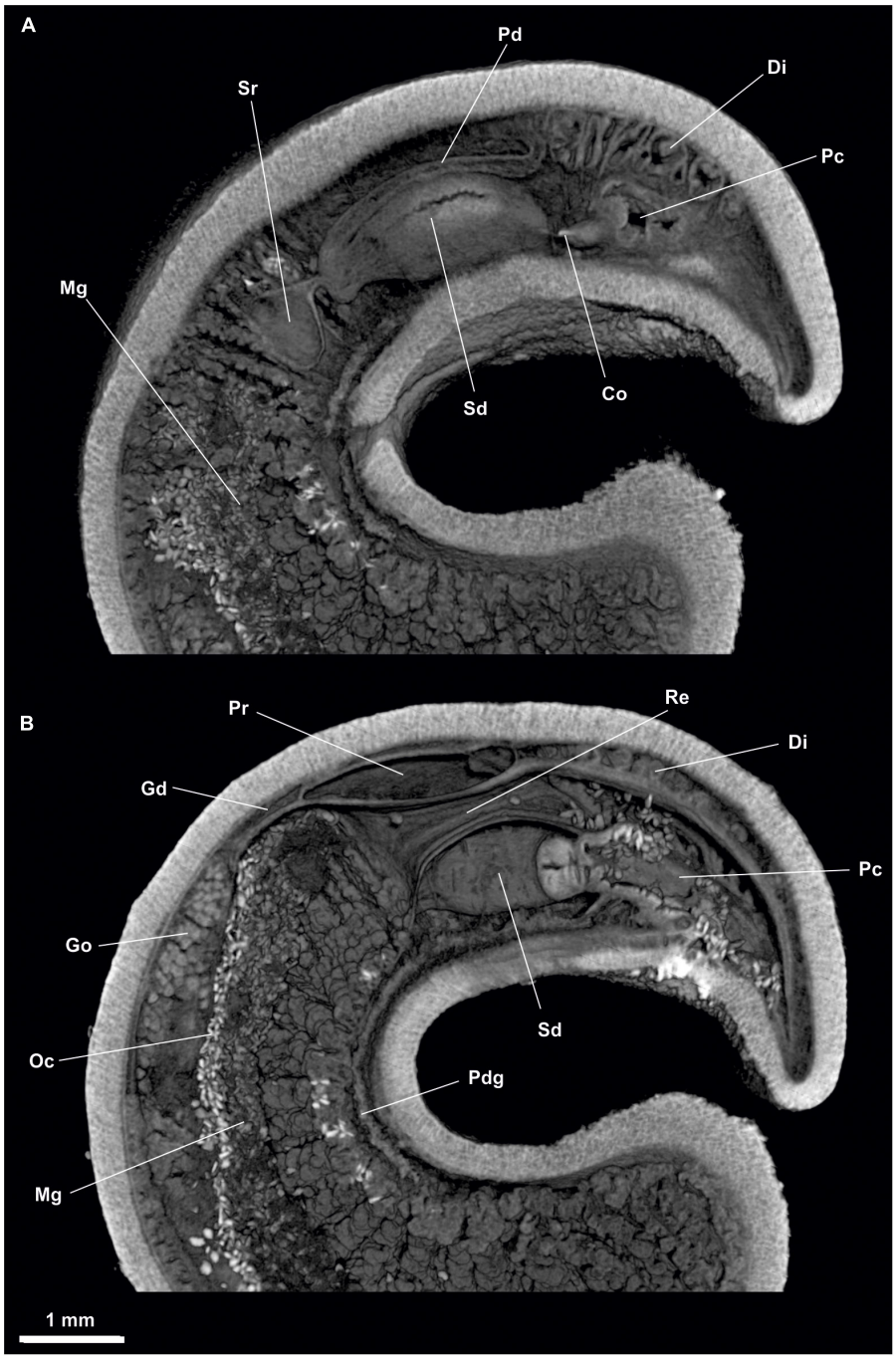


**FIGURE 9 |** *Dorymenia menchuescribanae*. **(A)** Sagittal view of the posterior body through spawning duct. **(B)** Sagittal view of the posterior body through rectum. Co, Copulatory stylets; Di, Diverticles; Gd, Gonopericardioduct; Go, Gonad; Mg, Midgut; Oc, Octocorallia; Pc, Pallial cavity; Pd, Pericardioduct; Pdg, Pedal gland; Pr, Pericardium; Re, Rectum; Sd, Spawning duct; Sr, Seminal receptacles.

Habitus.- Elongated body (**Figure 13A**), circular in section (30 mm long and 1 mm in diameter) with flattened ventral surface. Surface irregular, with interwoven acicular sclerites; some protruding from the mantle, giving the animal a hirsute appearance. Pedal groove (Pg, **Figures 13B,C**, **14E**, **15C,E**) visible from the outside (27 mm long), running ventrally from the pedal pit (Pp, **Figures 14A,D**), located posteriorly to the atriobuccal cavity, up to the pallial cavity without entering it. With scales on both sides of the pedal groove (**Figures 13B,C**).

Mantle.- Cuticle 80 μm thick. Acicular, interwoven sclerites (**Figure 13A**), some protruding from the mantle and projecting outwards. Elongated scales accompanying the pedal groove

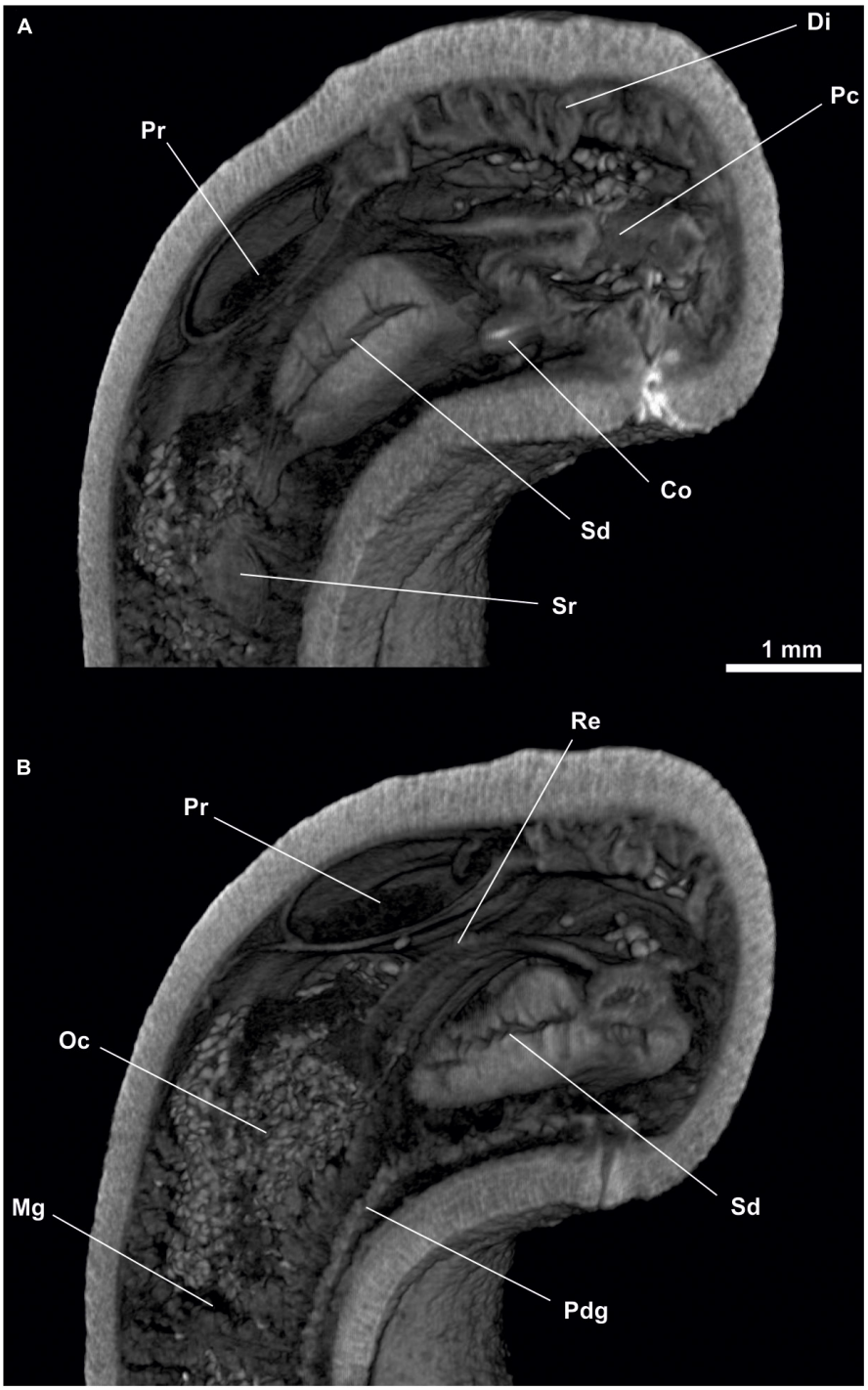


**FIGURE 10 |** *Dorymenia menchuescribanae*. **(A)** Cross-sagittal view through spawning duct. **(B)** Cross-sagittal view through rectum. Co, Copulatory stylets; Di, Diverticles; Mg, Midgut; Oc, Octocorallia; Pc, Pallial cavity; Pdg, Pedal gland; Pr, Pericardium; Re, Rectum; Sd, Spawning duct; Sr, Seminal receptacles.

along its entire length. No integumentary structures such as keels.

Pallial cavity.- The cavity (700 μm long and 400 μm in diameter) (Pc, **Figures 15A,B**) opens to the outside through a small opening, slightly wider than the pedal groove (700 μm long and 100 μm wide), in the ventroposterior region of the body. The pallial cavity bears marked diverticula (Di, **Figures 15B,C**) on the dorsal and lateral walls. The rostral region of the pallial cavity narrows slightly. The anus (150 μm in diameter) is located dorsorrostrally; the paired opening of the spawning ducts (Sdo,

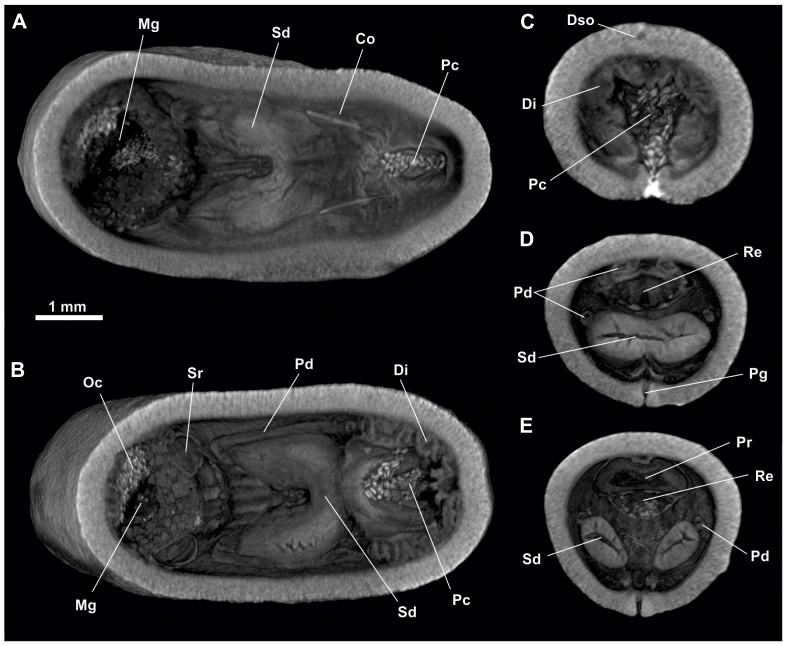


**FIGURE 11 |** *Dorymenia menchuescribanae*. **(A,B)** Dorsal view of the posterior body. **(C)** Cross-section of the posterior body through pallial cavity. **(D)** Cross-section of the posterior body through spawning duct opening and rectum. **(E)** Cross-section of the posterior body through pericardium. Co, Copulatory stylets; Di, Diverticles; Dso, Dorsoterminal sense organ; Mg, Midgut; Oc, Octocorallia; Pc, Pallial cavity; Pd, Pericardioduct; Pg, Pedal groove; Pr, Pericardium; Re, Rectum; Sd, Spawning duct; Sr, Seminal receptacles.

**Figures 15A–C**) (100 μm in diameter each) are located ventrally to the anus. The pallial cavity bears a ventrorrostral sac (Pvs, **Figure 15C**) projecting anteriorly (80 μm long and 100 μm in diameter) and abdominal spicules (Ab, **Figure 15A**).

Digestive system.- The atriobuccal cavity (500 μm long and 200 μm in diameter) opens to the outside through an opening 300 μm long, located in the ventroanterior region of the body. The mouth (Mo, **Figure 14B**) is located on the posterior wall of the atriobuccal cavity and is slightly flattened dorsoventrally (200 μm wide and 100 μm high). The pharynx (Ph, **Figures 14A,B,D**) is long and circular (1.3 mm long and 200 μm in diameter), has numerous glands on its dorsal wall, and a cuticle 25 μm thick. The ventral glandular organs of the pharynx (Vfg, **Figures 14A,E**) open onto the ventroposterior region of the pharynx and a little anterior to the radular sac (Rs, **Figure 14A**). These organs are of type B (García-Álvarez and Salvini-Plawen, 2007) and are formed by a pair of ducts 10 mm long and 80 μm in diameter, whose lumen is delimited by a muscular wall, and run ventrally to the intestine, intertwining on occasion. The pharynx (**Figures 14A,B,D**) enters ventrally into the intestine, it lacks an oesophagus. From the anterodorsal region of the intestine (Mg, **Figures 14A,B,E**), the dorsoanterior caecum (**Figures 14A,C,D**) projects, slightly flattened dorsoventrally (1.5 mm long, 150 μm wide and 100 μm high) reaching the height of the atriobuccal cavity. The dorsoventral musculature is visible (Dvm, **Figure 14E**). The intestine (Mg, **Figures 15B,E**) continues along the body (25 mm long and 500 μm in diameter) and ends in the rectum (Re, **Figures 15B,C**) (500 μm long and 150 μm in diameter), whose anus (150 μm in diameter) opens in the dorsorrostral wall of the pallial cavity.

Sense organs.- Small atrium (At, **Figures 14A,B**) (250 μm long, 200 μm wide and 200 μm high) occupying the anterior wall of the atriobuccal cavity (Abc, **Figure 14C**). The atrium bears thin, narrow-necked sensory papillary projections on the anterior, dorsal and lateral walls. The specimen has a dorsoterminal sense organ (Dso, **Figure 13C**) in the dorsal midline of the body, at the end of the pallial cavity, barely visible externally.

Gonopericardial system.- The pair of gonads (Go, **Figure 14B**) (24 mm long and 400 μm in diameter), have oocytes (Ov, **Figures 15D,E**) in the thin septum separating them. The gonopericardioducts (Gd, **Figure 15B**) (500 μm long and 300 μm in diameter) connect them to the rostral region of the pericardium (**Figure 15E**). The pericardium (Pr, **Figures 15D,E**) is wide (1 mm long and 600 μm in diameter) and has oocytes inside. The elongated and narrow heart (Ht, **Figure 15D**) is situated on its dorsal wall (1 mm long and 60 μm in diameter). The pericardium extends into two compartments posteriorly, from which both pericardioducts (Pd, **Figure 15D**) emerge from a laterotermINAL position; they run posteriorly, rotate, and run anteriorly along the sides of the body (1 mm long and 70 μm in diameter) and end in the anterior region of the spawning ducts (Sd, **Figures 15A,B,D**). The seminal receptacles (Sr, **Figures 15A,B,E**) form bundles (300 μm long and 150 μm in diameter as a whole), which end at the rostral wall of the spawning ducts, near the union with the pericardioducts. The two spawning ducts (1 mm long and 200 μm in diameter)

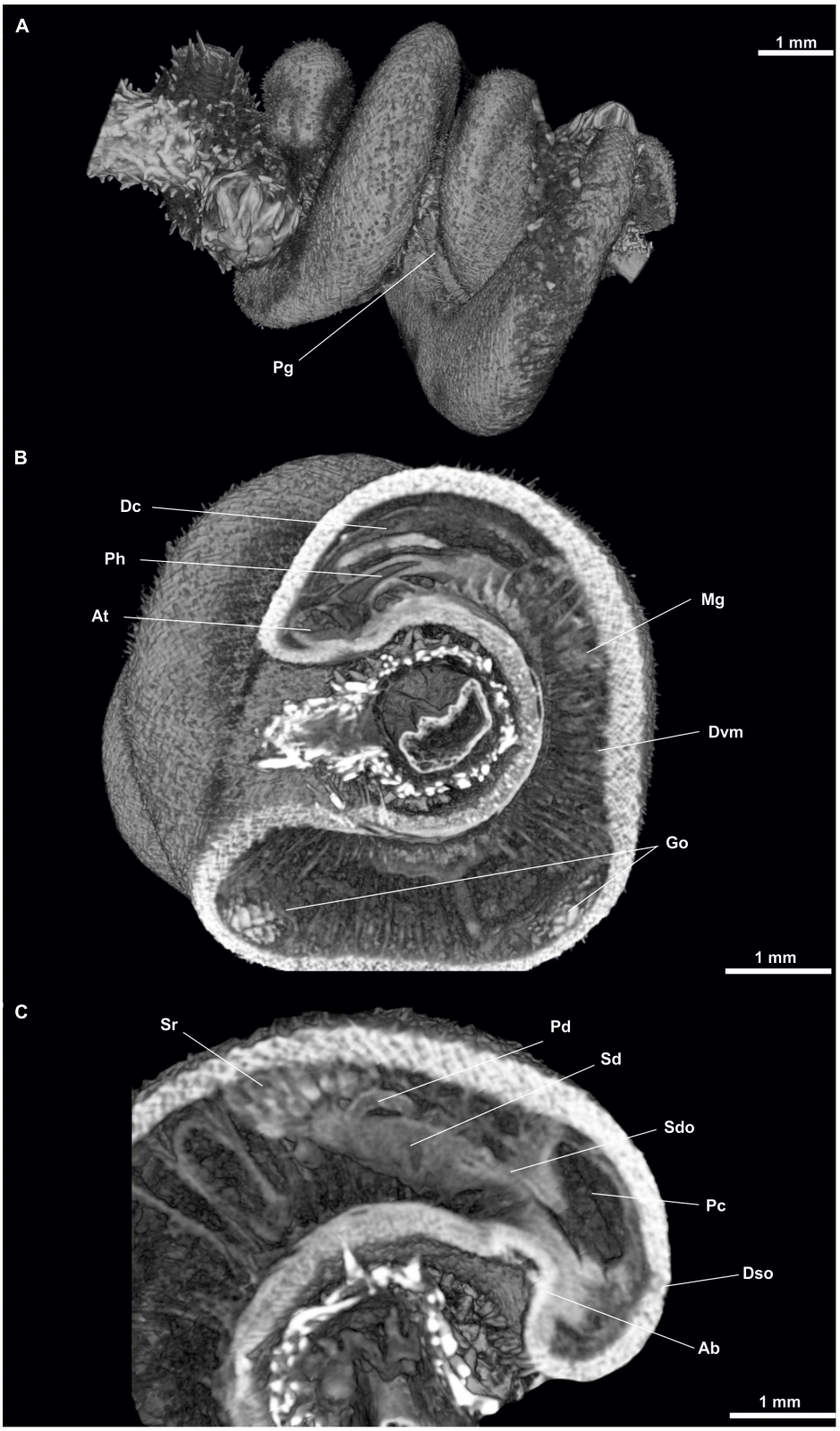


**FIGURE 12 |** *Anamenia gorgonophila* (Iceland). **(A)** Habitus. **(B)** Sagittal sections of the anterior body. **(C)** Sagittal view of posterior body through spawning duct. Ab, Abdominal spicules; At, Atrium; Dc, Dorsal caecum; Dvm, Dorsoventral musculature; Dso, Dorsoterminal sense organ; Go, Gonad; Mg, Midgut; Pc, Pallial cavity; Pg, Pedal groove; Ph, Pharynx; Sd, Spawning duct; Sdo, Spawning duct opening; Sr, Seminal receptacles.

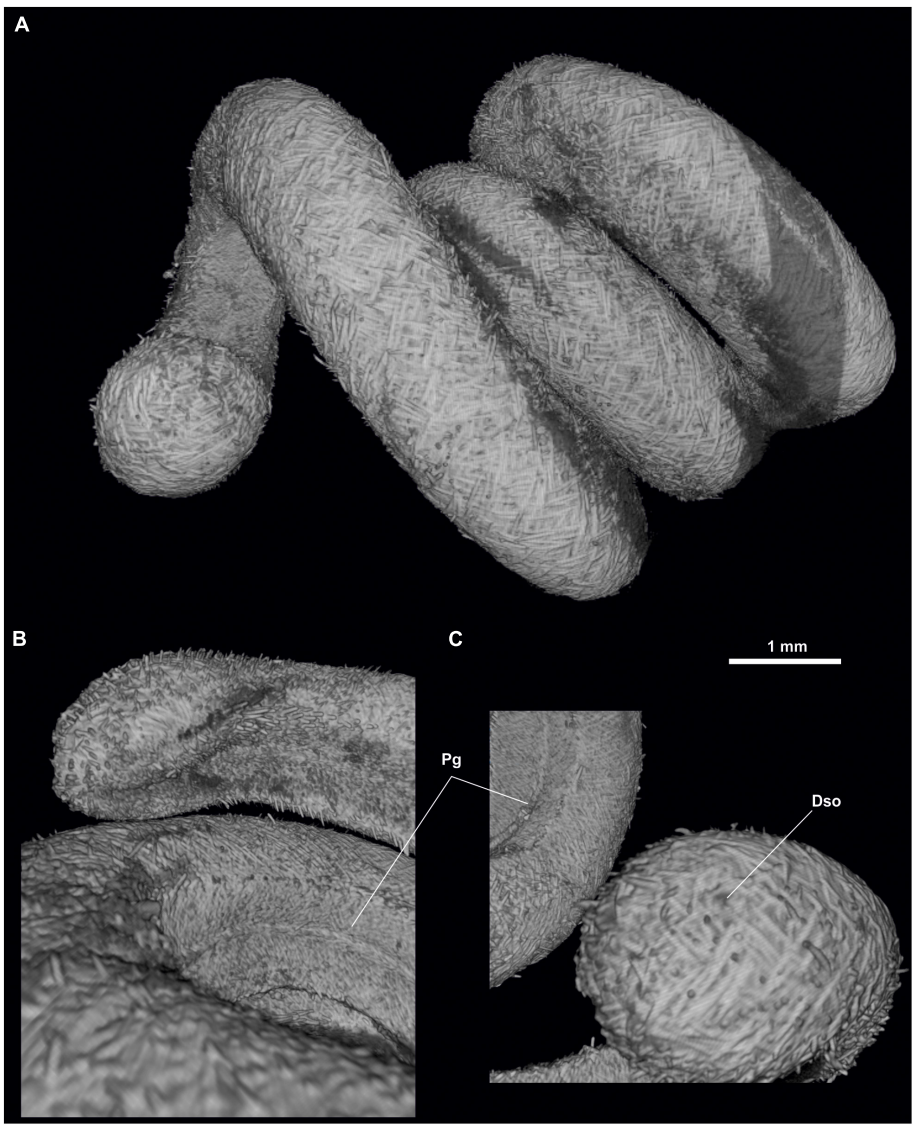


**FIGURE 13 |** *Anamenia gorgonophila* (Alborán). **(A)** Habitus. **(B)** Ventral view of the anterior body. **(C)** Dorsal view of the posterior body. Dso, Dorsoterminal sense organ; Mo, Mouth; Pc, Pallial cavity; Pg, Pedal groove.

run in a posterior direction, until they each lead individually (Sdo, **Figures 15A–C**) (100 μm in diameter) into the rostral wall of the pallial cavity, ventral to the anus and dorsal to the ventrorrostral sac.

## DISCUSSION

Here, we assessed the utility of micro-CT for the study of solenogaster internal anatomy and present the 3D internal anatomy the most taxonomically informative body regions of the four specimens studied. There are very few precedents in the use of this technique in the study of Solenogastres (Candás et al., 2018; Pedrouzo et al., 2019). Descriptions based on micro-CT images have not been performed in other Solenogastres species and are a good complementary tool to anatomical studies based on classical histological sections.

The specimen of *Proneomenia sluiteri* studied here comes from eastern Iceland (IceAGE Expedition), from a collection of 5 specimens presented at the 7th Congress of the European Malacological Societies. In the book of abstracts of the Congress they appear as *Dorymenia* sp., although in the posters that were presented, they were already correctly listed as *Proneomenia* sp. (Cobo et al., 2014; Pedrouzo et al., 2014a). These specimens were collected at the same IceAGE Expedition station as those studied and published by Todt and Kocot (2014). The description of the soft parts matches previously published descriptions (Hubrecht, 1880, 1881; Heuscher, 1892; Thiele, 1913; Todt and Kocot, 2014). The specimen studied measures 36 mm in length, within the range of 2–12 cm reported by Todt and Kocot (2014),

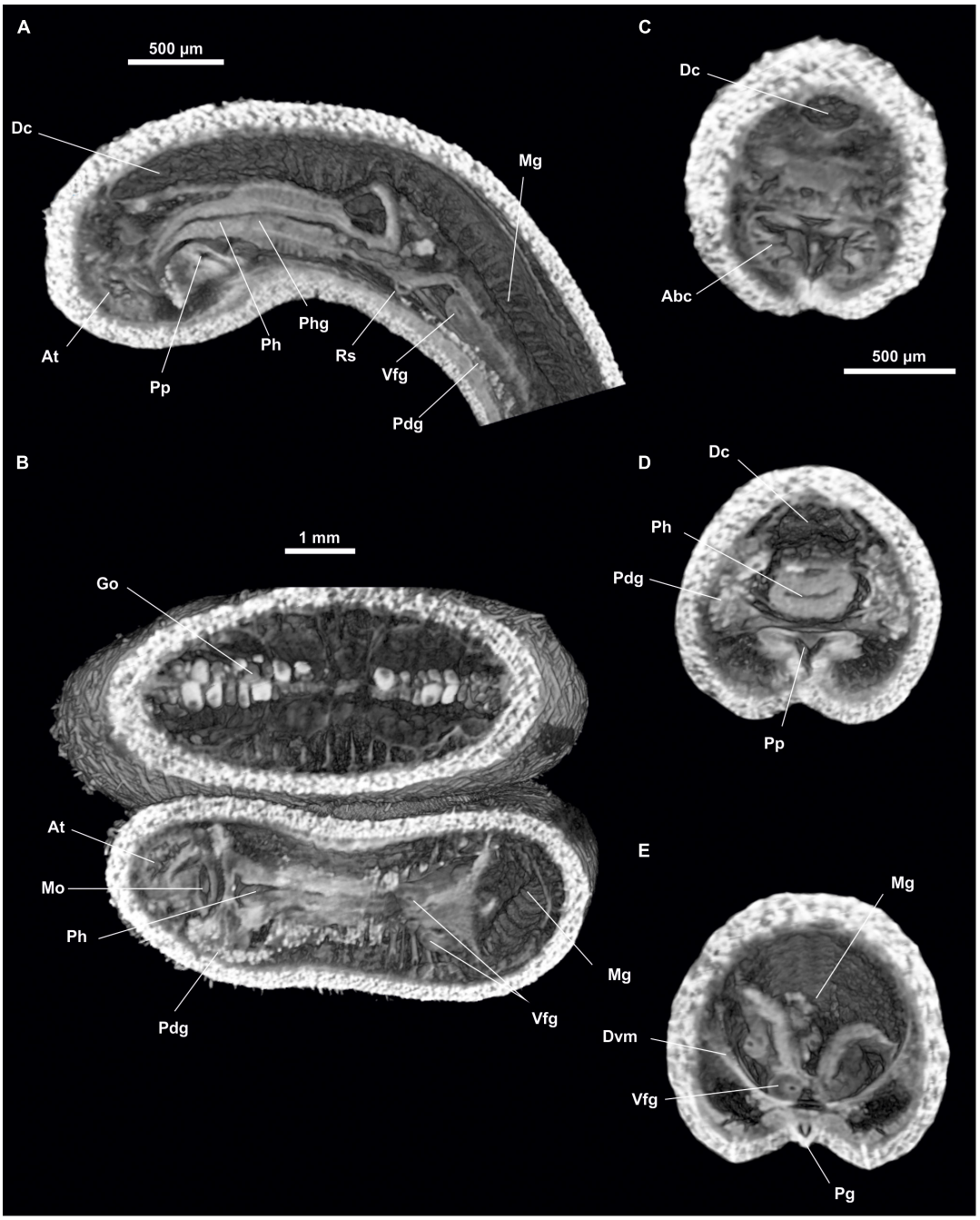


**FIGURE 14 |** *Anamenia gorgonophila* (Alborán). **(A)** Sagittal view of the anterior body through pharynx. **(B)** Dorsal view of the anterior body through atrium. **(C)** Cross section of the anterior body through atrium. **(D)** Cross section of the anterior body through pharynx. **(E)** Cross section of the anterior body through the midgut. Abc, Atriobucal cavity; At, Atrium; Dc, Dorsal caecum; Dvm, Dorsoventral musculature; Go, Gonad; Mg, Midgut; Mo, Mouth; Pdg, Pedal glands; Pg, Pedal groove; Ph, Pharynx; Phg, Pharynx glands; Pp, Pedal pit; Rs, Radular sack; Vfg, Ventral foregut glands.

or the 13 cm maximum length reported by Thiele (1913); it has an average diameter of 5 mm, also within the proportions stated by Thiele (1913), which indicates a diameter/length ratio of approximately 1:11. The cuticle is 250 µm thick, slightly thinner than other observations, which indicated 0.4 mm thickness (Thiele, 1913). The ventral glandular organs of the pharynx are 11 mm long and occupy 1/3 of the body length. It has an oesophagus, in agreement with other descriptions (Hubrecht, 1880, 1881). Intestinal contents have been observed, corresponding to Alcyonacea on which it feeds (Salvini-Plawen, 1972a). The seminal receptacles are elongated and undulating, and their attachment to the pericardioducts is observed very close

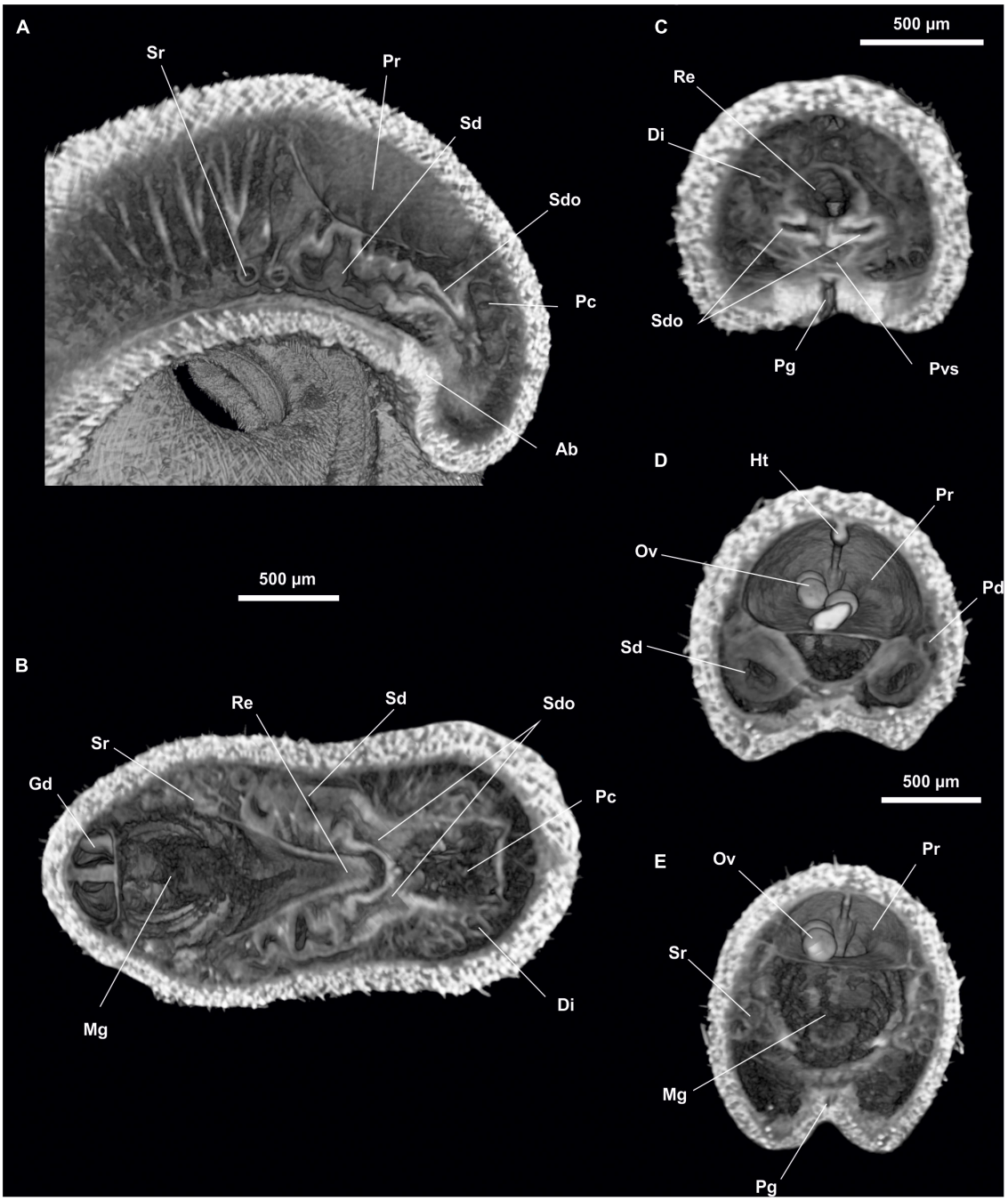


**FIGURE 15 |** *Anamenia gorgonophila* (Alborán). **(A)** Sagittal view of the posterior body through spawning duct. **(B)** Dorsal view of the posterior body through spawning ducts. **(C)** Cross section of the posterior body through spawning duct opening. **(D)** Cross section of the posterior body through spawning ducts. **(E)** Cross section of the posterior body through seminal receptacles. Ab, Abdominal spicules; Di, Diverticles; Gd, Gonopericardioduct; Ht, Heart; Mg, Midgut; Ov, Oocyte; Pc, Pallial cavity; Pd, Pericardioducts; Pg, Pedal groove; Pr, Pericardium; Pvs, Pallial cavity ventral sac; Re, Rectum; Sd, Spawning duct; Sdo, Spawning duct opening; Sr, Seminal receptacles.

to their point of attachment to the spawning ducts, although in other descriptions they have been observed just at the point of attachment (Todt and Kocot, 2014). The spawning ducts end oddly at the rostral wall of the pallial cavity. A dorso-terminal sensory organ is present.

The specimen studied here of *Dorymenia menchuescribanae*, paratype 1 of the type material and not cut in serial sections (García-Álvarez et al., 2000), matches the original description. The specimen measures 45 mm long, slightly less than in the original description, which states a range of 50–58 mm, but

within the range of 34–51 mm reported later for specimens from the same geographical area (García-Álvarez et al., 2009). The cuticle of 200–300 μm is within the range observed in García-Álvarez et al. (2009) (see **Figure 8**) although less thick than the original description where a thickness of 500 μm is indicated. Only 1 dorsoterminal sense organ was observed here, whereas previous descriptions indicated 2–4 organs (García-Álvarez et al., 2000, 2009). It has a preatrial sense organ located in the anterior wall of the atrium as noted by García-Álvarez et al. (2009). The ventral glandular organs of the pharynx are longer (30 mm in a 45 mm animal) than indicated, first third of the body, in the original description and their mouth is slightly anterior to the radular sac. The pericardium extends posteriorly into two compartments, not described above, from which each of the pericardioducts originates. The spawning duct leads unpaired onto the rostral wall of the ventral sac of the pallial cavity, as indicated in the original description, whereas in García-Álvarez et al. (2009) (see **Figure 11D**) it did so in a ventral position.

The description of the specimen of *Anamenia gorgonophila* collected in Iceland matches the original description. The specimen measures 30 mm long, 2 mm high and 1.5 mm wide and is slightly narrowed laterally. These measurements are in line with what has already been observed (Salvini-Plawen, 1972b; García-Álvarez et al., 1998; Pedrouzo et al., 2014b; Zamarro et al., 2015), although the lateral narrowing had not been noted. The cuticle measures 100–150 μm, thinner than reported by Pedrouzo et al. (2014b) and Zamarro et al. (2015) (200–220 μm), but slightly thicker than observed in García-Álvarez et al. (1998) (85–125 μm). It has 1 dorsoterminal sense organ, which is consistent with what had been previously described, 1–2 organs (Salvini-Plawen, 1972b; García-Álvarez et al., 1998; Zamarro et al., 2015). The seminal receptacles have been observed with difficulty to form bundles of 8, within the range of 6–15 already known (García-Álvarez et al., 1998; Zamarro et al., 2015). The two spawning ducts individually lead to the rostral wall of the pallial cavity, which is characteristic of this species (García-Álvarez et al., 1998; Zamarro et al., 2015).

The description of the specimen of *Anamenia gorgonophila* collected in Alboran Sea matches the original description. The specimen measures 30 mm long and 1 mm in diameter, with its ventral surface flattened; the measurements are within the range of other descriptions (Salvini-Plawen, 1972b; García-Álvarez et al., 1998; Pedrouzo et al., 2014b; Zamarro et al., 2015). The cuticle of this specimen is 80 μm thick, thinner than that indicated by García-Álvarez et al. (1998), 85–125 μm thick, and by Pedrouzo et al. (2014b) and Zamarro et al. (2015), which indicate a cuticle of 200–220 μm thick. Seminal receptacles are in bundles, 7 have been observed here with difficulty, similar to most descriptions indicating 6–15 per bundle (García-Álvarez et al., 1998; Zamarro et al., 2015).

The specimens were fixed in 70% ethanol as the mantle sclerites (which are calcium carbonate in composition) have to be preserved in good condition, as it is necessary to study the type of sclerites in the identification of Solenogastres. Furthermore, ethanol does not interfere with DNA sequencing and allows future molecular research on the same specimen that has been previously scanned.

Because the aim of this work was to study internal anatomy using three-dimensional models, these specimens were stained with iodine, which substantially increases the sharpness of the soft tissues in both 2D sections and 3D models. Iodine has been previously tested on other Solenogastres species (Pedrouzo et al., 2019). This compound stains virtually all tissue types, although it seems to have a preference for calcified structures and polysaccharides (Metscher, 2009; Faulwetter et al., 2013a). In images obtained in animals without iodine staining, it is not possible to visualise the internal anatomy. However, once stained, soft tissues are clearly visible (Candás et al., 2018). On the other hand, the sclerites are much clearer in the unstained specimens. In the iodine-treated specimens, the sclerites are covered by an excess of stain that was not removed by the ethanol rinse prior to dehydration with HMDS, which makes them appear too bright in the images and their arrangement is not clearly visible. This is clearly related to the preference of iodine for calcified structures.

The use of other stains such as phosphotungstic acid (PTA), phosphomolybdic acid (PMA) or osmium tetroxide have shown excellent results in other groups of Molluscs such as Bivalvia, Gastropoda, Scaphopoda and even Caudofoveata (Golding and Jones, 2007; Metscher, 2009; Faulwetter et al., 2013a; Candás et al., 2016, 2017; Marcondes Machado et al., 2018; Ziegler et al., 2018). Osmium tetroxide is a very toxic compound, so its use in this study was discarded. As for PTA, we have performed different tests with Solenogastres whose results show that it is not a good stain in the study of these animals as it seems to destroy the sclerites, possibly due to its acidic nature (Candás et al., 2018; Kocot, unpublished data). Another advantage of iodine staining is that it is possible to extract nucleic acids from specimens after scanning (Green et al., 2017).

Computed microtomography or micro-CT made it possible to study most of the anatomical structures of the specimens under study, which have a relatively large size in relation to the small average size of Solenogastres. With this technique it was possible to obtain 2D images that adequately complement those obtained by means of serial histological sections, and also a very relevant 3D view of the internal anatomical structure, which allowed both precise measurements and observation of the relative position of the organs with different focus and angles. However, it was not possible to observe the radula, possibly due to its small size. The observation of ventral foregut organs by micro-CT is not easy. In the specimens studied here, which are relatively large, it was possible to observe them and determine their type. However, in other small-sized specimens, the observation of these organs is difficult, even impossible in some cases, especially if the organs are small like clustered-type, type A or *Simrothiella*-like (Pedrouzo et al., 2019). Neither was it possible to visualise the nervous system, nor to clearly define the glandular structures. In other larger marine molluscs (Cephalopoda) it has been possible to see the nervous structures using PTA as a contrast agent (Ziegler et al., 2018). Despite some limitations, results of this study highlight micro-CT as a valuable

tool for the non-destructive study of solenogaster morphology. In particular, it is very useful for identifying animals to the family and even genus level, which allows us to start identification or classification work by means of classical histological techniques without destroying the specimens.

Hence, Micro-CT is proved to be a very useful tool for an initial, quick, non-destructive approximation for most of the internal structures of Solenogastres, making it possible to reach family or even genus taxonomic level. Nonetheless, histology is still required for the description of small or glandular parts, which are important for species-level identification in many cases. Therefore, these techniques remain complementary.

## DATA AVAILABILITY STATEMENT

Data are available through the following link in morphosource: https://www.morphosource.org/projects/000384772.

## AUTHOR CONTRIBUTIONS

JM-S, KK, ÓG-Á, MC, and GD-A: anatomical study, figure production, article redaction, and images production with micro-CT. All authors contributed to the article and approved the submitted version.

## FUNDING

KK received funding from the United States National Science Foundation (NSF DEB 1846174).

## ACKNOWLEDGMENTS

We would like to thank the scientists and crew of the Me-85/IceAGE cruise, the DZMB, and Senckenberg. We would also like to acknowledge the University of Alabama Water Institute for their contribution to the fee for publishing this article.

## REFERENCES

Alba-Tercedor, J., and Sánchez-Tocino, L. (2011). The use of the SkyScan 1172 high resolution micro-CT to elucidate if the spicules of the sea slugs (Mollusca: Nudibranchia, Opisthobranchia) have a structural or a defensive function. *Skyscan Users Meet* 2011, 113–121.

Candás, M., Díaz-Agras, G., Abad, M., Barrio, L., Cunha-Veira, X., Pedrouzo, L., et al. (2016). Application of micro-CT in the study of the anatomy of small marine molluscs. *Microsc. Anal.* 30, S8–S11.

Candás, M., Díaz-Agras, G., García-Álvarez, O., and Urgorri, V. (2018). "Study of the applicability of micro-CT for identification of *Mollusca Solenogastres*," in *Proceedings of the Bruker Micro-CT User Meeting Abstract Book*, Ghent, 32–40.

Candás, M., Díaz-Agras, G., and Urgorri, V. (2017). "First steps in morphological analysis of the of the reproductive system of *Doto pinnatifida* (Montagu,1804)," in *Proceedings of the Bruker Micro-CT User Meeting Abstract Book*, Brussels, 112–116.

Cobo, M. C., Pedrouzo, L., Candás, M., García-Álvarez, O., and Urgorri, V. (2014). "The use of Micro-CT vs classical histological techniques in the study of the internal anatomy of Solenogastres," in *Proceedings of the 7th Congress of the European Malacological Societies, Conference Programme & Book of Abstracts*, ed. T. S. White (Bruges: Cambridge).

Faulwetter, S., Vasileiadou, A., Kouratoras, M., Dailianis, T., and Arvanitidis, C. (2013b). Micro-computed tomography: introducing new dimensions to taxonomy. *Zookeys* 263, 1–45. doi: 10.3897/zookeys.263.4261

Faulwetter, S., Dailianis, T., Vasileiadou, A., and Arvanitidis, C. (2013a). Contrast enhancing techniques for the application of micro-CT in marine biodiversity studies. *Microsc. Anal.* 27, S4–S7. doi: 10.1007/978-3-319-17001-5_53-1

García-Álvarez, O., and Salvini-Plawen, L. (2007). Species and diagnosis of the families and genera of *Solenogastres* (Mollusca). *Iberus* 25, 73–143.

García-Álvarez, O., Salvini-Plawen, L., and Urgorri, V. (2014). "Solenogastres," in *Mollusca, Solenogastres, Caudofoveata, Monoplacophora*, Vol. 38, eds O. García-Álvarez, L. Salvini-Plawen, V. Urgorri, J. S. Troncoso, F. Ibérica, and M. Ramos (Madrid: Museo Nacional de Ciencias Naturales), 31–163.

García-Álvarez, O., Urgorri, V., and Cristobo, F. J. (1998). Sobre la presencia de Anamenia gorgonophila (Kowalevsky, 1880) (Mollusca, Solenogastres: Cavibelonia) en las costas de la Península Ibérica. *Nova Acta Científ. Compost.* 9, 249–258.

García-Álvarez, O., Urgorri, V., and Salvini-Plawen, L. (2000). Two new species of *Dorymenia* (Mollusca: Solenogastres: Proneomeniidae) from the South Shetland Islansds (Antarctica). *J. Mar. Biol. Assoc. U. K.* 80, 835–842. doi: 10.1017/S0025315400002812

García-Álvarez, O., Zamarro, M., and Urgorri, V. (2009). Proneomeniidae (Solenogastres, Cavibelonia) from the Bentart-2006 Expedition, with description of a new species. *Iberus* 27, 67–78.

Gignac, P. M., Kley, N. J., Clarke, J. A., Colbert, M. W., Morhardt, A. C., Cerio, D., et al. (2016). Diffusible iodine-based contrast-enhanced computed tomography (diceCT): an emerging tool for rapid, high-resolution, 3-D imaging of metazoan soft tissues. *J. Anat.*. 228, 889–909. doi: 10.1111/joa.12449

Golding, R. E., and Jones, A. S. (2007). Micro-CT as a novel technique for 3D reconstruction of molluscan anatomy. *Mollusc. Res.* 27, 123–128.

Green, R. M., Leach, C. L., Hoehn, N., Marcucio, R. S., and Hallgrímsson, B. (2017). Quantifying three-dimensional morphology and RNA from individual embryos. *Dev. Dyn.* 246, 431–436. doi: 10.1002/dvdy.24490

Heuscher, J. (1892). Zur anatomie und histologie der proneomenia sluiteri hubrecht. *Jenaische Zeitschr. Nat.* 27, 477–512.

Hubrecht, A. A. W. (1880). Proneomenia sluiteri, gen. et sp. n. eine neue archaische Molluskenform aus dem Eismeere. *Zool. Anzeig.* 3, 589–590.

Hubrecht, A. A. W. (1881). Proneomenia sluiteri, gen. et sp. n. with remarks upon the anatomy and histology of the Amphineura. *Niederl. Arch. Zool.* 2, 1–75.

Keklikoglou, K., Faulwetter, S., Chatzinikolaou, E., Wils, P., Brecko, J., Kvaček, J., et al. (2019). Micro-computed tomography for natural history specimens: a handbook of best practice protocols. *Eur. J. Tax.* 522, 1–55. doi: 10.5852/ejt.2019.522

Kocot, K. M., Todt, C., Mikkelsen, N. T., and Halanych, K. M. (2019). Phylogenomics of Aplacophora (Mollusca, Aculifera) and a solenogaster without a foot. *Proc. R. Soc. B* 286:20190115. doi: 10.1098/rspb.2019.0115

Kowalevsky, A. (1880). Ueber die bau und die lebensersegeinungen von *Neomenia gorgonophilus*. *Zool. Anz.* 3, 190–191.

Marcondes Machado, F., Dias Passos, F., and Giribet, G. (2018). The use of micro-computed tomography as a minimally invasive tool for anatomical study of bivalves (*Mollusca: Bivalvia*). *Zool. J. Linn. Soc.* 186, 46–75. doi: 10.1093/zoolinnean/zly054

Metscher, B. D. (2009). MicroCT for comparative morphology: simple staining methods allow high-contrast 3D imaging of diverse non-mineralized animal tissues. *BMC Physiol.* 9:11. doi: 10.1186/1472-6793-9-11

Nierstrasz, H. (1908). The Solenogastres of the discovery-expedition. *Nat. Antarct. Exp. 1901–1904 Nat. Hist.* 4, 38–46.

Paterson, G. L., Sykes, D., Faulwetter, S., Merk, R., Ahmed, F., Hawkins, L. E., et al. (2014). The pros and cons of using micro-computed tomography in gross and

micro-anatomical assessments of polychaetous annelids. *Mem. Mus. Victor.* 71, 237–246. doi: 10.24199/j.mmv.2014.71.18

Paz-Sedano, S., Candás, M., Gosliner, T. M., and Pola, M. (2021). Undressing *Lophodoris danielsseni* (Friele & Hansen, 1878) (Nudibranchia: Goniodorididae). *Organ. Divers. Evol.* 21, 107–117. doi: 10.1007/s13127-020-00470-z

Pedrouzo, L., Cobo, M. C., García-Álvarez, O., Rueda, J. L., Gofas, S., and Urgorri, V. (2014a). Solenogastres (*Mollusca*) from expeditions off the South Iberian Peninsula, with the description of a new species. *J. Nat. Hist.* 48, 2985–3006. doi: 10.1080/00222933.2014.959576

Pedrouzo, L., Cobo, M. C., Señarís, M. P., García-Álvarez, O., and Urgorri, V. (2014b). "A deep-sea Dorymenia sp. (*Mollusca, Solenogastres*) from East Iceland, Norwegian Sea (IceAGE-project)," in *Proceedings of the 7th Congress of the European Malacological Societies, Conference Programme & Book of Abstracts*, ed. T. S. White (Cambridge: The Malacological Society of London).

Pedrouzo, L., García-Álvarez, O., Urgorri, V., and Pérez-Señarís, M. (2019). New data and 3D reconstruction of four species of *Pruvotinidae* (Mollusca: Solenogastres) from the NW Iberian Peninsula. *Mar. Biodivers.* 49, 277–287. doi: 10.1007/s12526-017-0793-1

Salvini-Plawen, L. (1972b). Revision der monegassischen solenogastres (Mollusca, Aculifera). *J. Zool. Syst. Evol. Res.* 10, 215–240. doi: 10.1111/j.1439-0469.1972.tb00799.x

Salvini-Plawen, L. (1972a). Cnidaria as food-sources for marine invertebrates. *Cah. Biol. Mar.* 13, 385–400.

Salvini-Plawen, L. V. (1978). Antarktische und subantarktische Solenogastres. *Zoologica* 128, 1–305.

Simroth, H., and Bronn, H. G. (1893). *Klassen und Ordnungen des Tierreichs*.

Thiele, J. (1913). "Solenogastres," in *Friedländer und Sohn*, ed. D. Tierreich (Berlin: Verlag von R), 1–57. doi: 10.5962/bhl.title.51964

Todt, C., and Kocot, K. M. (2014). New records for the solenogaster *Proneomenia sluiteri* (Mollusca) from Icelandic waters and description of Proneomenia custodiens sp. n. *Pol. Polar Res.* 35, 291–310. doi: 0.2478/popore-2014-0012

Urgorri, V., Señarís, M. P., Díaz-Agras, G., Candás, M., and Gómez-Rodríguez, C. (2021). Doris adrianae sp. nov. (Heterobranchia; Nudibranchia; Doridina) from the Galician coasts (NW Iberian Peninsula). *Nova Acta Científ. Compost.* 28, 1–33.

Zamarro, M., García-Álvarez, O., and Urgorri, V. (2015). New anatomical and biogeographical data on solenogastres cavibelonia from the Galician Continental margin (NW Spain). *Iberus* 33, 1–26.

Ziegler, A., Bock, C., Ketten, D. R., Mair, R. W., Mueller, S., Nagelmann, N., et al. (2018). Digital three-dimensional im-aging techniques provide new analytical pathways for malacological research. *Am. Malacol. Bull.* 36, 248–273. doi: 10.4003/006.036.0205

**Conflict of Interest:** The authors declare that the research was conducted in the absence of any commercial or financial relationships that could be construed as a potential conflict of interest.

**Publisher's Note:** All claims expressed in this article are solely those of the authors and do not necessarily represent those of their affiliated organizations, or those of the publisher, the editors and the reviewers. Any product that may be evaluated in this article, or claim that may be made by its manufacturer, is not guaranteed or endorsed by the publisher.